DOI 10.1007/s11106-021-00183-8
Powder Metallurgy and Metal Ceramics, Vol. 59, Nos. 9-10, January, 2021 (Russian Original Vol. 59, Nos. 9-10, Sept.-Oct., 2020)

EXCHANGE OF EXPERIENCE

EFFECT OF SELECTIVE LASER MELTING PARAMETERS ON THE MELT POOL FORMED BY SINGLE TRACKS OF THE HEAT-RESISTANT INCONEL 718 NICKEL ALLOY

S.V. Adjamsky,[1,2] Yu.V. Tkachev,[1]
and G.A. Kononenko[2–4]

UDC 621.7: 62-293

The characteristics of single-track melt pools, such as size, shape, and stability, formed by the heat-resistant Inconel 718 nickel alloy powder subjected to selective laser melting (SLM) were studied. The objective was to determine the range of optimal SLM parameters to provide a stable track with a depth of two to three layers. Single tracks were built using various combinations of process parameters: laser power from 50 to 400 W with a step of 30 W and scanning speed from 450 to 1000 mm/sec with a step of 50 mm/sec (144 modes in total). An Axiovert 200M MAT light microscope (Carl Zeiss) was employed to examine the cross sections of single tracks and evaluate the geometrical parameters of the melt pools. Features pertaining to the effect of the scanning speed and laser power on single-track depth and width and their ratio were experimentally studied. An unstable track formed at low power (P = 50 W) and low scanning speed (V = 450–500 mm/sec), while no track appeared at all at higher speeds. A stable track formed at power P = 80–200 W at low speeds (V = 500–900 mm/sec) and became unstable and intermittent when speed increased to V = 1000 mm/sec. With higher laser power (P = 230–400 W) and low process speeds, a continuous track formed but had an increased variable width, being indicative of a deviation from the stable track formation conditions. It was first established that the intensity of the scanning speed effect (450–1000 mm/sec) on the single track depth varies by more than 2.5 times depending on the laser power (50–400 W). The process parameters that would ensure the formation of an optimal single track in terms of geometric parameters were determined.

Keywords: *selective laser melting, Inconel 718, single track, melt pool geometry, optimum conditions.*

[1]Oles Honchar Dnipro National University, Dnipro, Ukraine; [2]LLC Additive Laser Technology of Ukraine, Dnipro, Ukraine. [2]LLC 'Additive Laser Technology of Ukraine', Dnipro, Ukraine. [3]Nekrasov Institute of Iron and Steel, National Academy of Sciences of Ukraine, Dnipro, Ukraine.

[4]To whom correspondence should be addressed; e-mail: dsit@dnu.edu.ua, office.isi@nas.gov.ua.

Translated from Poroshkova Metallurgiya, Vol. 59, Nos. 9–10 (535), pp. 137–147, 2020. Original article submitted October 21, 2019.

INTRODUCTION

The method of selective laser melting (SLM) allows forming products layer by layer and creating, thus, the parts of complex geometric shapes, whose manufacture was previously expensive or impossible by standard technologies. High tensile strength, fracture toughness, and wear resistance at relatively high temperatures make the Inconel 718 alloy composed of 0.50–0.55% Ni, 17–21% Cr, 4.75–5.5% Nb, and 2,8–3.3% Co quite attractive for use under high temperatures, wear, and an aggressive media (these are, in particular, turbines, nuclear reactors, jet engines, and combustion chambers). At the same time, these properties make further processing of the product extremely difficult [1–3].

Hence, the SLM method is highly relevant for the production of parts from the Inconel 718 alloy. This is one of the few commercially attractive additive manufacturing techniques that can be used to obtain parts from nickel-based alloys with a porosity closed to zero [4–6]. The SLM technology uses a localized and focused laser beam for melting powder particles to form a liquid metal pool of micron sizes, which subsequently solidifies at high speed, forming a layer.

The process functional diagram for the 3D printer is presented in Fig. 1. Such equipment allows creating component parts of complex geometry in layers through melting using a digital 3D model as source information. The thickness of the layer varied between 15 and 150 μm depending on the material. Ytterbium fiber lasers with a power of 200 to 1000 W were used to melt metal in powder form. The radiation focuses on the desired place to form the contour of the workpiece using high-speed drive mirrors [7, 8]. The chamber is filled with inert gas (nitrogen or argon) to prevent the undesirable oxidation during production. Each following layer is achieved by lowering the platform with the workpiece to the height of the layer. Next, a new powder layer is applied from the hopper using a drive blade. The whole cycle is repeated until the part is fully formed in height.

During selective laser melting, metal powders melt rapidly within the layer under the action of a laser beam that moves at high speed, and then quickly solidify in the melt pool (cooling rate varies between 10^3 and 10^8 K/sec [9]) with short-term nonequilibrium phase transition, forming a highly dispersed microstructure.

The effect of the melt pool parameters on the quality of 3D parts construction from different materials was studied in detail [10–13]. It was established that the small size of the melt pool reduces the process efficiency due to

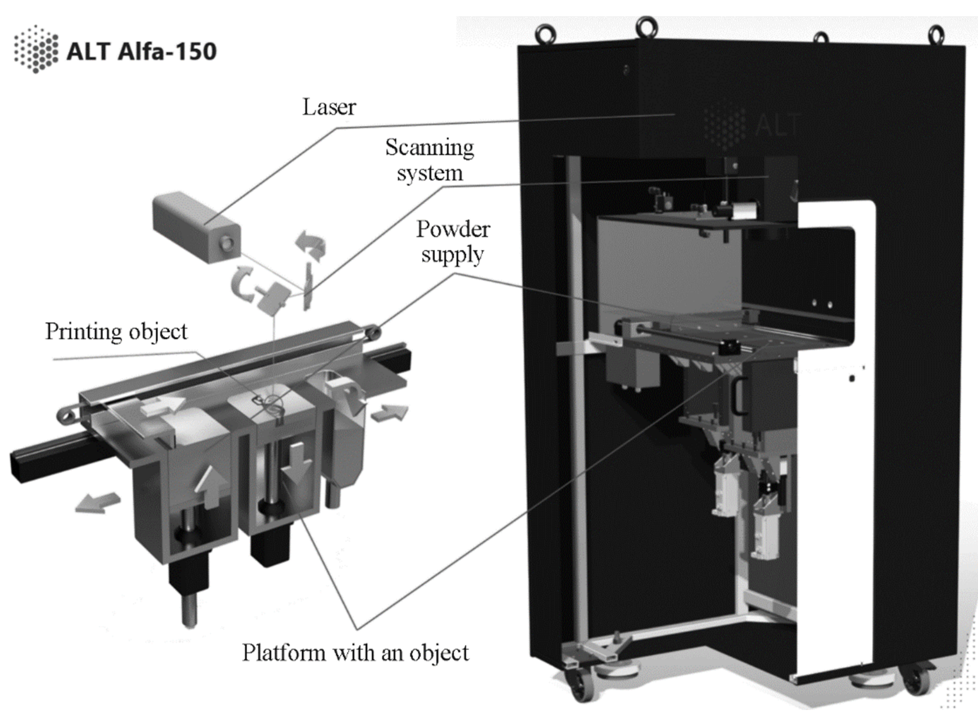

Fig. 1. Schematic diagram of the 3D printer

the increase in manufacturing time. A large melt pool can increase production efficiency, but at the same time cause the substrate or powder to evaporate, which will lead to the formation of pores and increase the overall porosity of the materials [11, 14]. Therefore, the quality of the product, including the final density and surface roughness, primarily depends on the characteristics of the melt pool (shape and size), which are largely controlled by changes in the energy density of the laser beam. Basically, it is a measure of the energy supplied during processing. Energy density is controlled by changing the appropriate controlled parameters. Laser power P (W), scanning speed V (mm/sec), the distance between tracks (melt pool overlap) d (mm), and layer thickness t (mm) are the most important parameters related to the laser energy density [14, 15]: $E = P / (V \cdot d \cdot t)$. It is important to develop rational modes that would provide a satisfactory level of quality of the details and efficiency of the technological process.

ANALYSIS OF RESEARCH IN RECENT YEARS

Studies by Gu et al. [15] conducted on stainless steel have shown that such parameters as laser power and scanning speed have different effects on the porosity and evolution of the microstructure. Ian et al. [16] proved experimentally that the quality of the product primarily depends on the scanning speed, laser power, and layer thickness. The relative significance of each process parameter was examined by statistical analysis, and the scanning speed was found to be the most affecting parameter [17]. The low scanning speed ensures complete melting of the particles and provides a dense structure, but the efficiency of the process is significantly reduced. At very low scanning speeds, the instability of the melt pool causes uneven melting along each track, which leads to high surface roughness and higher bulk porosity due to the formation of bubbles [10, 11]. At higher scanning speeds, the short-term interaction between the material and the laser beam facilitates the formation of narrow melt pools, which also increases the surface roughness [11]. Furthermore, very high scanning speeds can increase the porosity and incite the formation of thermal cracks due to high cooling rates [18]. Therefore, the search for the optimal scanning speed is a compromise between the performance and quality of the product manufacture process.

The influence of Inconel 718 laser melting [12, 19–21] on microstructural transformations and related changes in the mechanical properties of the product has been sufficiently studied. However, studies on the effect of changes in laser processing parameters on the porosity and microstructure of the Inconel 718 alloy are very poor [22]. According to the study results of the samples produced at different scanning speeds and varying combinations of laser power, the alloy compaction is associated with the laser energy density, and the maximum product density is achieved at its optimum values. However, the efficiency of the main process parameters, such as laser power, scanning speed, and general scanning strategy, on the porosity and microstructure of the alloy is not fully disclosed in this study.

Therefore, our goal was to examine the influence of the selective laser melting process parameters (laser power and scanning speed) on the characteristics of the melt pool (depth, width, and the ratio between them) for the Inconel 718 alloy. The data obtained will also enable the determination of the optimum technological SLM modes in the production of three-dimensional products from Inconel 718 with the desired density and microstructure.

MATERIALS AND METHODS

The material used to produce samples by the SLM method was an AMPERPRINT 0181.074 powder of Inconel 718 alloy (HC Starck) with a particle size of –45+15 μm. The source material (shape and particle size) was examined under the REM-106 scanning electron microscope (Fig. 2).

The experiment was conducted on an ALT Alfa-150 unit produced by LLC Additive Laser Technology of Ukraine in a protective nitrogen atmosphere. The device was equipped with a ytterbium laser with a power of up to 500 W, and the printing area was 150 mm × 150 mm × 180 mm. We obtained single tracks at different combinations of laser power and scanning speed. A typical single track is repeated with a clearly defined overlap to complete the detail. Some studies on single tracks were performed on a base-plate made of another alloy [23]. However, such experimental conditions provide changes in the chemical composition due to the dilution (mixing)

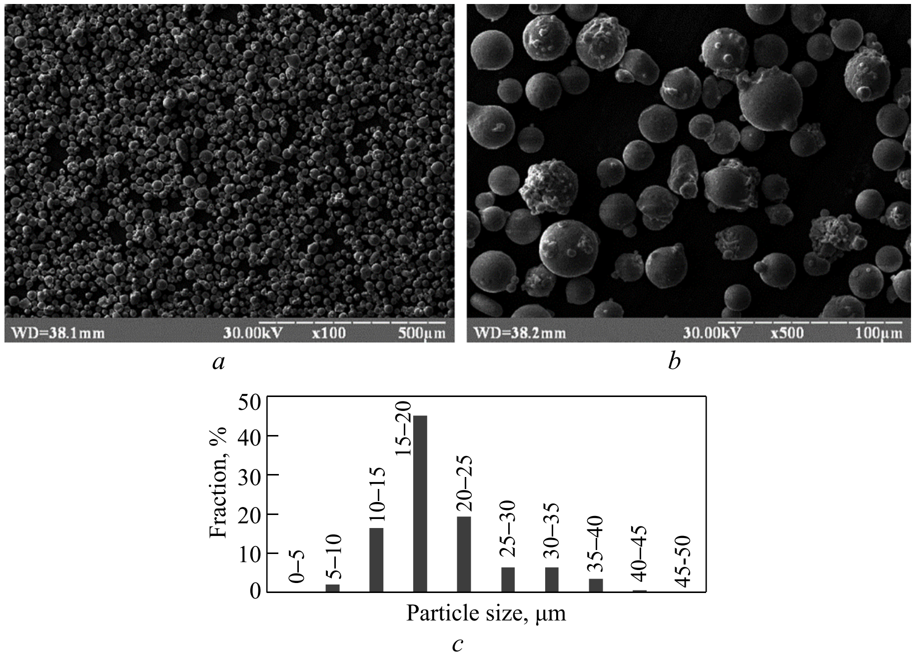

Fig. 2. Particles of the Inconel 718 source material at a magnification of 100 (*a*) and 500 (*b*); results of particle size distribution analysis (*c*)

of the test material and the metal of the base-plate, leading to changes in the melting temperature of the powder alloy.

This paper introduces a different approach to the production of a single track, namely, by creating it on a base platform made of the same material. The power varied between 50 and 400 W with a step of 30 W, and the speed was changed in the range of 450–1000 mm/sec with a step of 50 mm/sec. A total of 144 single track modes located between 1.5 and 2 mm from each other were examined. There were six groups of three single tracks per block (Fig. 3) produced in the same mode. The thickness of the layer used in the experiments was 50 μm.

Surface morphology, dimensions of individual tracks, cross-sectional area and geometric parameters (Fig. 4) of the melt pool were characterized by an Axiovert 200M MAT (Carl Zeiss) light microscope.

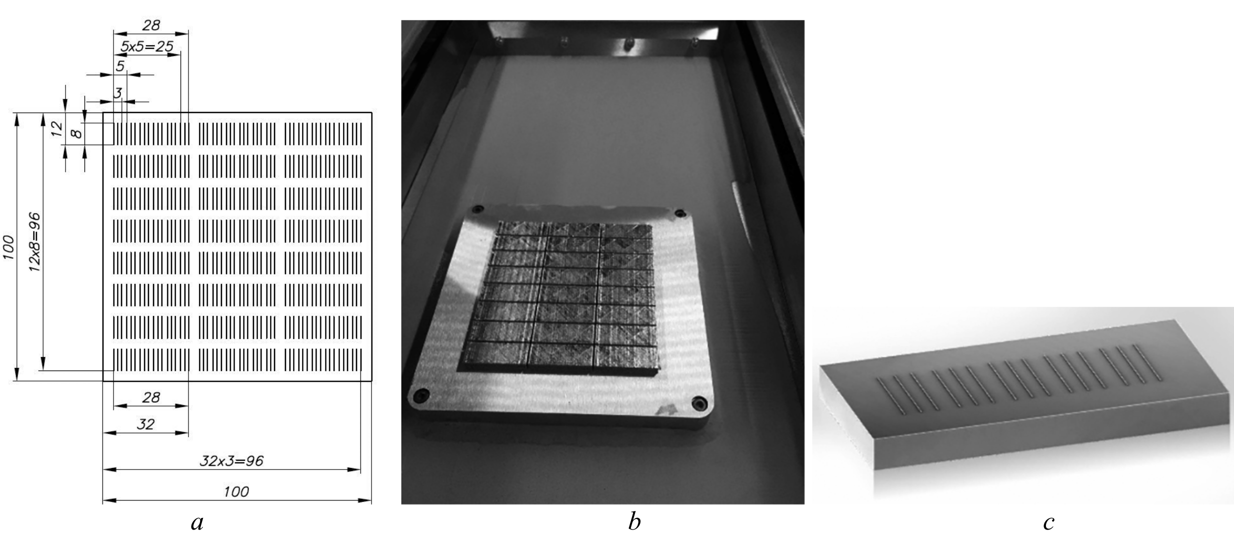

Fig. 3. Arrangemnet pattern of single tracks built at different modes (*a*), general view of the site with samples in the working chamber (*b*), isometric view of the site with single tracks (*c*)

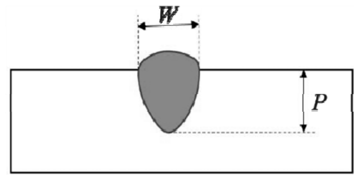

Fig. 4. Single-track geometry: W is track width, P is track depth

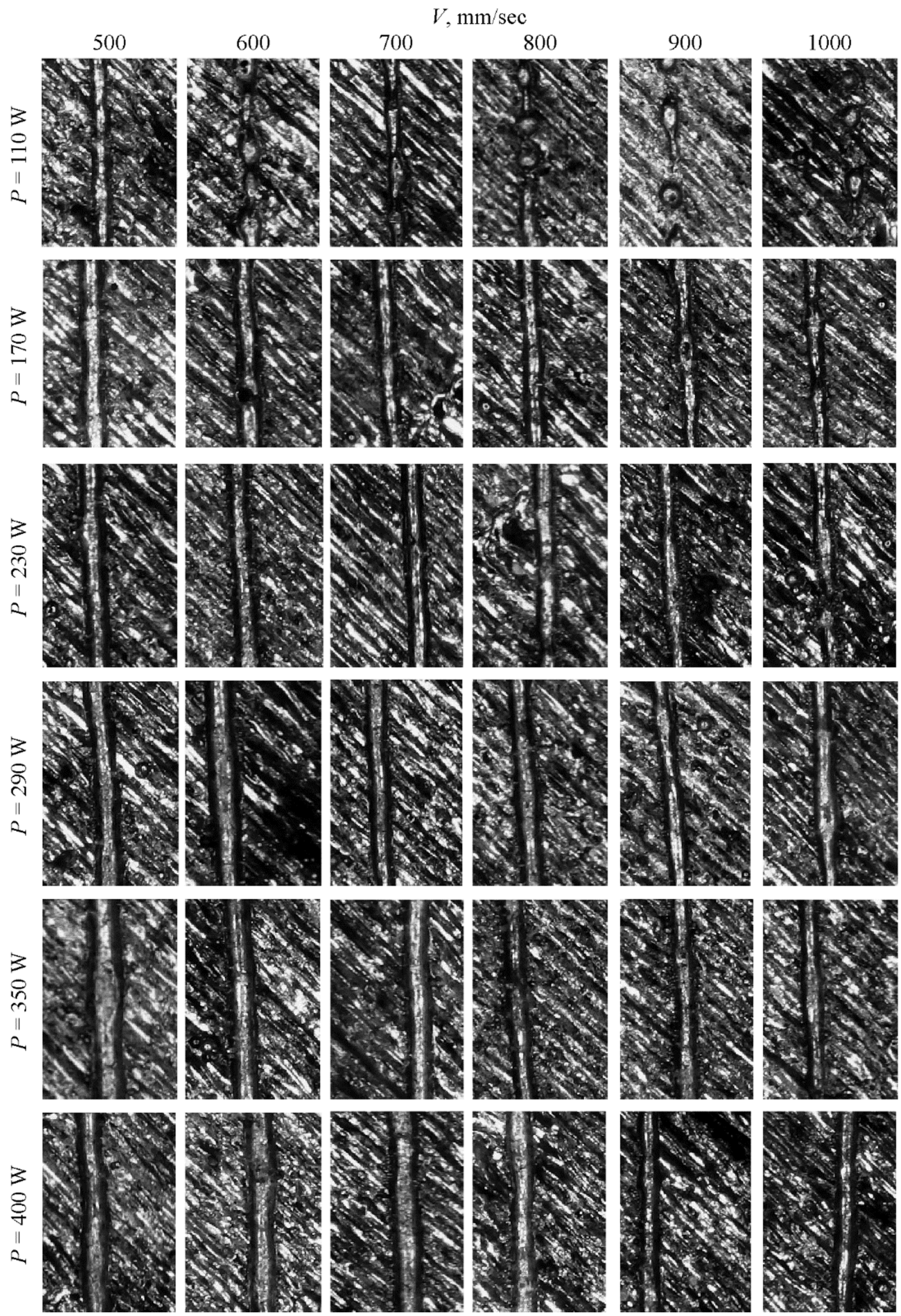

Fig. 5. General profile of a single track produced on the substrate

RESEARCH RESULTS

The appearance of some studied single tracks is demonstrated in Fig. 5. At low power (P = 50 W) and low scanning speed (V = 450–500 mm/sec), an unstable track was formed, while at higher speeds, no tracks were formed at all.

At power P = 80–200 W, a stable track was formed at low speeds, becoming unstable and intermittent with a higher speed (Fig. 5). With a further increase in laser power (P = 230–400 W) and at low processing speeds, a high-quality track was formed, but with increasing the scanning speed, a decrease in its width was observed (Fig. 5). The results on evaluating the stability of the resulting tracks by appearance are given in the Table 1. However, in SLM, the melting depth must not exceed the thickness of the two layers. To determine the working window of the process, i.e., modes in which a stable track is formed, it is necessary to set the geometric dimensions of the melt pool for each of the modes.

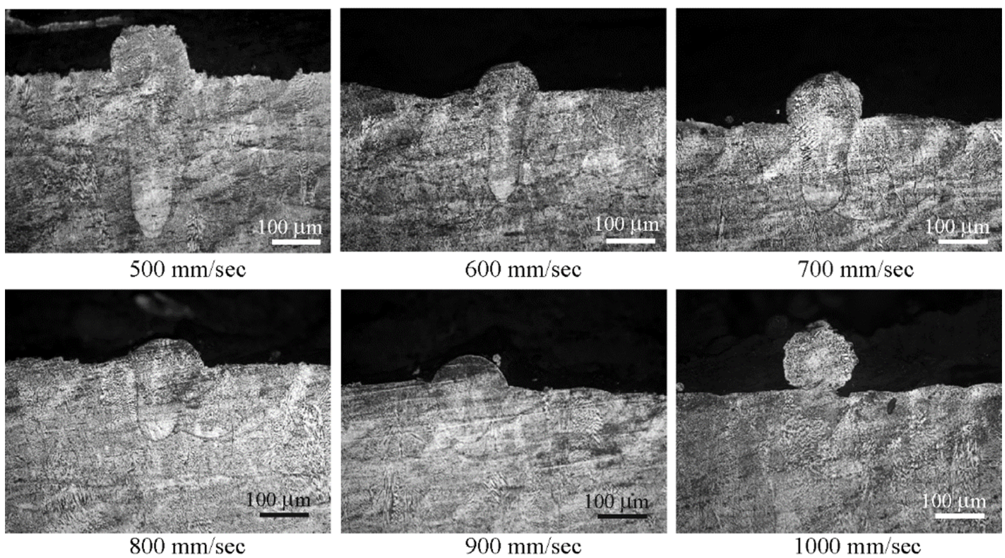

Fig. 6. Cross-sectional microstructure of single tracks formed on the substrate at a laser power of P = 200 W and different scanning speeds

TABLE 1. Stability of Single Tracks under Different Laser Power and Scanning Speed

Power, W	Speed, mm/sec											
	450	500	550	600	650	700	750	800	850	900	950	1000
50	UNS	UNS	N/F	N/F	N/F	N/F	N/F	N/F	N/F	N/F	N/F	N/F
80	UNS	UNS	UNS	UNS	UNS	UNS	UNS	UNS	UNS	UNS	UNS	UNS
110	ST	ST	UNS	UNS	UNS	UNS	UNS	UNS	UNS	UNS	UNS	UNS
140	ST	ST	ST	ST	ST	UNS	UNS	UNS	UNS	UNS	UNS	UNS
170	ST	ST	ST	ST	ST	ST	ST	ST	ST	UNS	UNS	UNS
200	ST	ST	ST	ST	ST	ST	ST	ST	ST	ST	UNS	UNS
230	ST	ST	ST	ST	ST	ST	ST	ST	ST	ST	ST	ST
260	ST	ST	ST	ST	ST	ST	ST	ST	ST	ST	ST	ST
290	ST	ST	ST	ST	ST	ST	ST	ST	ST	ST	ST	ST
320	ST	ST	ST	ST	ST	ST	ST	ST	ST	ST	ST	ST
350	ST	ST	ST	ST	ST	ST	ST	ST	ST	ST	ST	ST
400	ST	ST	ST	ST	ST	ST	ST	ST	ST	ST	ST	ST

Notes: N/F—not formed; UNS—unstable, ST—stable track.

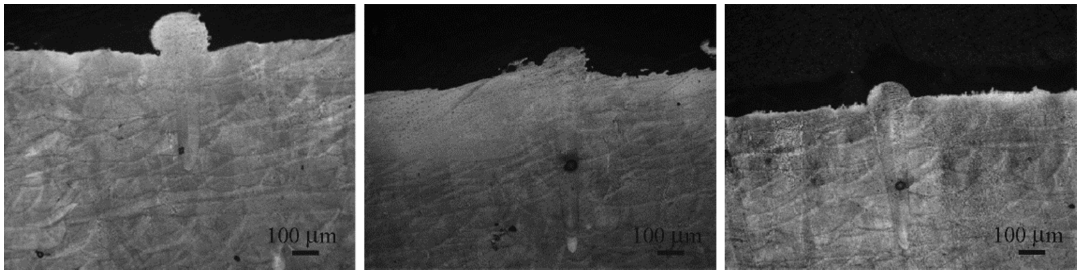

a *b* *c*

Fig. 7. The cross-sectional microstructure of the tracks formed on the substrate: *a*) $P = 400$ W, $V =$ $= 500$ mm/sec; *b*) $P = 400$ W, $V = 450$ mm/sec; *c*) $P = 350$ W, $V = 450$ mm/sec

Figure 6 illustrates the microstructure of the experimental tracks at different scanning speeds and constant laser power ($P = 200$ W). At a speed of 1000 mm/sec, an unstable track is formed, and droplet formation occurs, as follows from Fig. 6. In other words, being of low temperature, the molten metal does not spread on the substrate.

The microstructure of the tracks formed under the modes with sufficiently high power and low scanning speed is shown in Fig. 7. As can be seen, the depth of the pool of a single track exceeds the optimal values of 2–3 layers.

Afterward, geometric dimensions of single tracks were calculated. The average width and depth values for the single track pool are shown on Fig. 8. The results indicate that the scanning speed significantly affects the change of geometric parameters of the track pool, and this effect is more pronounced for the depth of the track rather than for its width. The depth-to-width ratio of a single-track pool is shown in Fig. 9.

The results indicate that laser power and scanning speed have a major impact on track depth. With high energy density (high power and low speed), there is a deeper penetration, which can reach between 5 and 25 layers. In such a case, the same microvolume of metal is subjected to repeated melting, which negatively affects the quality of the metal. In addition, at a large depth of the melt pool, and, hence, its large volume, the temperature gradient between the cooled metal of the lower layers and the liquid metal of the upper layers is quite significant. As a consequence, the microstructure becomes coarse grained and high stresses occur, leading to microcracks in some

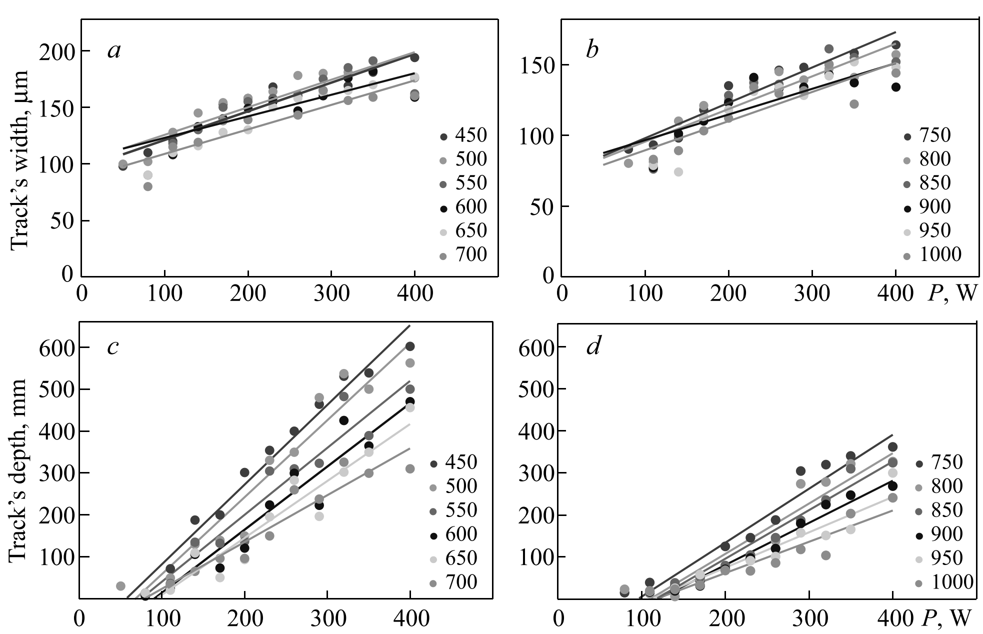

Fig. 8. Width (*a, b*) and depth (*c, d*) of a single track under different laser power (80–400 W) and scanning speeds of 450–700 (*a, c*) and 750–1000 mm/sec (*b, d*)

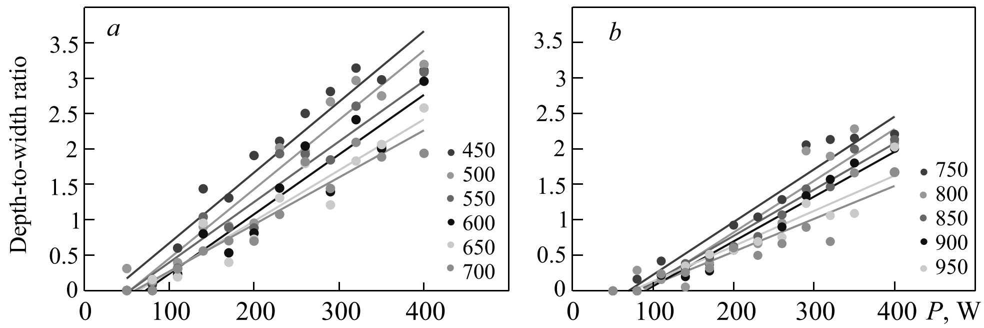

Fig. 9. The depth-to-width ratio of a single track under different laser power (80–400 W) and scanning speeds of 450–700 (*a*) and 750–950 mm/sec (*b*)

cases. Moreover, under deep melting, the track acquires an elongated form, the depth-to-width ratio changes, and typical defects known in the literature as 'keyhole' are observed (Fig. 7). Externally, the track in this sector seems stable, with almost no external defects. However, due to the descent of the hole, large pores are formed along the entire track in the depth of its cross-section, which is an irreparable defect in the printed part.

CONCLUSIONS

The single tracks of the Inconel 718 alloy, layered under different modes of the selective laser melting process, have been investigated to understand their influence on the features of the melt pool. Such studies of single tracks can reduce scope of process parameters and improve time-consuming experiments to develop efficient process modes.

Experimental dependences of change in depth and width values of a single-track pool at various combinations of laser power and scanning speed have been established. It has been shown that the effect intensity of changing the scanning speed was more pronounced on the depth of a single-track pool rather than the change in power.

The optimal operational modes have been determined, providing a penetration depth of not more than two layers and a wide melt pool (with a ratio of the melt pool depth to its width of not more than 2). These parameters indicated adequate wettability of the substrate surface, leading to minimal internal structural defects and low surface roughness.

The results obtained could serve as a basis for future modelling of the selective laser melting process at various combinations of laser power and scanning speed. Likewise, the results can be useful for determining the optimum modes of creating a single layer to produce high-quality three-dimensional parts.

REFERENCES

1. A.R.C. Sharman, A. Amarasinghe, and K. Ridgway, "Tool life and surface integrity aspects when drilling and hole making in Inconel 718," *J. Mater. Process Technol.,* **200**, 424–432 (2008).
2. A.K. Parida and K. Maity, "Comparison the machinability of Inconel 718, Inconel 625 and Monel 400 in hot turning operation," *Eng. Sci. Technol. Int. J.,* **21**, 364–370 (2018).
3. N. Narutaki, Y. Yamane, K. Hayashi, and T. Kitagawa, "High-speed machining of Inconel 718 with ceramic tools," *CIRP Annals.*, **42**, 103–106 (1993).
4. Y.M. Arisoy, L.E. Criales, T. Özel, and B. Lane, "Influence of scan strategy and process parameters on microstructure and its optimization in additively manufactured nickel alloy 625 via laser powder bed fusion," *Int. J. Adv. Manuf. Technol.,* **90**, 1393–1417 (2017).
5. L.E. Criales, Y.M. Arisoy, B. Lane, and T. Özel, "Laser powder bed fusion of nickel alloy 625: Experimental investigations of effects of process parameters on melt pool size and shape with spatter analysis," *Int. J. Mach. Tools Manuf.,* **121**, 22–36 (2017).

6. X. Wang, X. Gong, and K. Chou, "Review on powder-bed laser additive manufacturing of Inconel 718 parts," *Proc. Inst. Mech. Eng. B J. Eng. Manuf.,* **231**, 1890–1903 (2017).
7. C.B. Williams, F. Mistree, and D.W. Rosen, "Towards the design of a layerbased additive manufacturing process for the realization of metal parts of designed mesostructured," in: *Proc. 16th Solid Freeform Fabrication Symposium* (2005), p. 217–230.
8. Concept Laser GmbH [electronic resource], Access: https://www.concept-laser.de/technologie.html.
9. L.-E. Loong, C.-K. Chua, W.-Y. Yeong, J. Song, M. Mapar, S.L. Sing, Zh.-H. Liu, and D.-Q. Zhang, "Numerical investigation and an effective modelling on the Selective Laser Melting (SLM) process with aluminium alloy 6061," *Int. J. Heat Mass. Transf.*, **80**, 288–300 (2015).
10. K. Kempen, L. Thijs, E. Yasa, M. Badrossamay, and J.-P. Kruth, "Process optimization and microstructural analysis for selective laser melting of AlSi10Mg," in: *Solid Freeform Fabrication Symposium* (2011), pp. 484–495.
11. C. Kamath, B. Eldasher, G.F. Gallegos, W. King, and A. Sisto, "Density of additively-manufactured, 316L SS parts using laser powder-bed fusion at powers up to 400 W," *Int. J. Adv. Manuf. Technol.,* **74**, 65–78 (2014).
12. Q. Jia and D. Gu, "Selective laser melting additive manufacturing of Inconel 718 superalloy parts: densification, microstructure and properties," *J. Alloys Compd.*, **585**, 713–721 (2014).
13. B. Song, S. Dong, H. Liao, C. Coddet, "Process parameter selection for selective laser melting of Ti6Al4V based on temperature distribution simulation and experimental sintering," *Int. J. Adv. Manuf. Technol.,* **61**, 967–974 (2012).
14. J.J.S. Dilip, S. Zhang, C. Teng, K. Zeng, C. Robinson, D. Pal, and B. Stucker, "Influence of processing parameters on the evolution of melt pool, porosity, and microstructures in Ti–6Al–4V alloy parts fabricated by selective laser melting," *Prog. Additive Manuf.*, **2**, 157–167 (2017).
15. H. Gu, H. Gong, D. Pal, H. K. Rafi, T. Starr, and B. Stucker, "Influences of energy density on porosity and microstructure of selective laser melted 17-4PH stainless steel," in: *Solid Freeform Fabrication Symposium* (2013), p. 474–489.
16. J. Yang, J. Han, H. Yu, J. Yin, M. Gao, Z. Wang, X. Zeng, "Role of molten pool mode on formability, microstructure and mechanical properties of selective laser melted Ti–6Al–4V alloy," *Mater. Des.,* **110**, 558–570 (2016).
17. C. Kamath, "Data mining and statistical inference in selective laser melting," *Int. J. Adv. Manuf. Technol.,* **86**, 1659–1677 (2016).
18. W.J. Sames, F. List, S. Pannala, F.A. List, and R.R. Dehoff, "The metallurgy and processing science of metal additive manufacturing," *Int. Mater. Rev*., **61**, 315–360 (2016).
19. K.N. Amato, S.M. Gaytan, L. E. Murr, E. Martinez, P.W. Shindo, J. Hernandez, S. Collins, and F. Medina, "Microstructures and mechanical behavior of Inconel 718 fabricated by selective laser melting," *Acta Mater.,* **60**, 2229–2239 (2012).
20. M. Pröbstle, S. Neumeier, J. Hopfenmüller, L.P. Freund, T. Niendorf, D. Schwarze, and M. Göken, "Superior creep strength of a nickel-based superalloy produced by selective laser melting," *Mater. Sci. Eng. A.,* **674**, 299–307 (2016).
21. G.E. Bean, D.B. Witkin, T.D. McLouth, and R.J. Zaldivar, "The effect of laser focus and process parameters on microstructure and mechanical properties of SLM Inconel 718," *Int. Soc. Optics Photonics*., **10523**, 105230Y (2018).
22. J.-P. Choi, G.-H. Shin, S. Yang, D.-Y. Yang, J.-S. Lee, M. Brochu, and J.-H. Yuad, "Densification and microstructural investigation of Inconel 718 parts fabricated by selective laser melting," *Powder Technol.,* **310**, 60–66 (2017).
23. Haijun Gong, Hengfeng Gu, Kai Zeng, J.J.S. Dilip, Deepankar Pal, and Brent Stucker, "Melt pool characterization for selective laser melting of Ti–6Al–4V pre-alloyed powder," in: *Solid Freeform Fabrication Symposium* (2014), p. 256–267.